J. Mol. Biol. (1994) 238, 264–280

Salt Effects on Protein–DNA Interactions

The λcI Repressor and *Eco*RI Endonuclease

Vinod K. Misra[1], Jonathan L. Hecht[1], Kim A. Sharp[2]
Richard A. Friedman[1] and Barry Honig[1]†

[1]*Department of Biochemistry and Molecular Biophysics*
Columbia University, New York, NY 10032, U.S.A.

[2]*Department of Biochemistry and Biophysics*
University of Pennsylvania, Philadelphia, PA 19104. U.S.A.

In this paper, finite-difference solutions to the nonlinear Poisson–Boltzmann (NLPB) equation are used to calculate the salt dependent contribution to the electrostatic DNA binding free energy for both the λcI repressor and the *Eco*RI endonuclease. For the protein–DNA systems studied, the NLPB method describes nonspecific univalent salt dependent effects on the binding free energy which are in excellent agreement with experimental results. In these systems, the contribution of the ion atmosphere to the binding free energy substantially destabilizes the protein–DNA complexes. The magnitude of this effect involves a macromolecular structure dependent redistribution of both cations and anions around the protein and the DNA which is dominated by long range electrostatic interactions. We find that the free energy associated with global ion redistribution upon binding is more important than changes associated with local protein–DNA interactions (ion-pairs) in determining salt effects. The NLPB model reveals how long range salt effects can play a significant role in the relative stability of protein–DNA complexes with different structures.

Keywords: DNA; electrostatics; DNA binding; binding energy; salt

1. Introduction

Proteins interact with nucleic acids to control gene regulation and expression. In order to understand these control processes in atomic detail, the structural and energetic basis for the specificity and stability of binding must be elucidated. Structural analyses of protein–DNA complexes suggest that binding free energies depend on direct interactions involving both polar and nonpolar contacts as well as indirect interactions involving conformation dependent effects on long range forces such as electrostatics and salt effects (Harrison & Aggarwal, 1990). The binding free energy of protein–DNA complexes depends strongly on salt concentration (Record *et al.*, 1978, 1985, 1991). For example, increasing the NaCl concentration from 0·10 to 0·15 M decreases the binding constant of the *lac* repressor protein with DNA by almost two orders of magnitude (deHaseth *et al.*, 1977; Riggs *et al.*, 1970). Furthermore, salt dependent effects can play a significant role in the site specific binding of several proteins to DNA (Koblan & Ackers, 1991*a*; Senear & Batey, 1991; Terry *et al.*, 1983). The linkage between electrolyte activity and binding is related to the energetics of the interaction of the small ions with the macromolecules.

Salt effects in nucleic acid systems are often treated with the "standard" model in which DNA is described as an isolated, infinitely long, uniformly charged cylinder in solvent modeled as a structureless continuum (Anderson & Record, 1990). In this model, the binding of a Z-valent ligand is described by the neutralization of Z charges on the cylindrical polyion (Anderson & Record, 1982, 1983; Manning, 1978; Record *et al.*, 1978). The neutralization of charges changes the interaction of the DNA with the small ions resulting in the salt dependence of binding.

The standard model can be developed in terms of counterion condensation (CC‡) theory (Manning, 1969, 1978) and Poisson–Boltzmann (PB) theory

† Author to whom all correspondence should be addressed.

‡ Abbreviations used: CC, counterion condensation; PB, Poisson–Boltzmann; NLPB, nonlinear Poisson–Boltzmann; MC, Monte Carlo simulation; FDPB, finite difference Poisson–Boltzmann; CVFF, consistent valence force field; RMSD, root-mean-square deviation; WT, wild-type.

0022-2836/94/170264-17 $08.00/0

formulated as the electroneutral cell model (Marcus, 1955; Alfrey *et al.*, 1951; Fuoss *et al.*, 1951) or the full NLPB model with added salt (Misra *et al.*, 1994). The essential difference in the description of salt effects between the CC and PB theories is the description of the radial distribution of small ions around the nucleic acid. The CC theory models the counterion atmosphere around DNA as two distinct populations: a salt invariant "condensed" layer bound within a well-defined volume around the polyion; and a salt dependent Debye–Hückel layer which is treated as a classical ion atmosphere. In contrast, the PB theory models the counterion atmosphere around a polyion as a single population described by a continuously distributed salt dependent ion atmosphere. These differences have been shown to result in very different thermodynamic descriptions of salt dependent effects in nucleic acid equilibria (Misra *et al.*, 1994). The CC model typically describes salt effects in terms of the cratic entropy of ion release (Manning, 1978; Record *et al.*, 1976), while the PB model emphasizes the role of long range electrostatic interactions (Misra *et al.*, 1994).

Although CC and cylindrical PB cell models have been remarkably successful in describing the interactions of small ions with rod-like polyions, these standard models do not explicitly account for the detailed molecular structures and charge distributions of ligand–DNA systems. Their applicability may then be limited in systems which significantly deviate from simple cylindrical geometries. In systems with complicated shapes and charge distributions, such as protein–DNA complexes, simple cylindrical models cannot make quantitative thermodynamic predictions. A theory that specifically relates a molecule's three-dimensional shape and charge distribution to its free energy is clearly needed.

Accurate descriptions of the electrostatic properties of a variety of complex macromolecules are given by finite difference solutions to the PB equation (Honig *et al.*, 1993). Furthermore, the total electrostatic free energy for any system modeled with the full nonlinear PB (NLPB) equation has been unambiguously defined (Reiner & Radke, 1990; Sharp & Honig, 1990*a*). Thus, the electrostatic contribution of macromolecule–solvent and macromolecule–small ion interactions to protein–DNA binding energies can be calculated from finite difference solutions to the NLPB equation for detailed molecular geometries.

Salt effects on ligand–DNA interactions result from changes in the macromolecule–small ion interaction free energy upon binding (Misra *et al.*, 1994). In NLPB theory, the macromolecule–small ion interaction free energy is described by three terms: an electrostatic ion–molecule interaction free energy, $\Delta\Delta G^{\circ}_{im}$; an electrostatic ion–ion interaction free energy, $\Delta\Delta G^{\circ}_{ii}$; and an entropic ion organization free energy, $\Delta\Delta G^{\circ}_{org}$. The salt dependent variation in these three terms has been shown to describe accurately the salt dependence of the experimentally observed binding constant for several minor groove binding antibiotics. In each case, salt effects are dominated by $\Delta\Delta G^{\circ}_{im}$ (Misra *et al.*, 1994). In addition, the finite difference NLPB model has been shown to accurately reproduce the salt dependence of the binding free energy of the λcI repressor–operator interaction (Zacharias *et al.*, 1992). However, this analysis did not present a physical description of salt dependent effects on protein binding in terms of NLPB theory.

Monte Carlo (MC) simulations including detailed atomic level structures have also been used to analyze the salt dependence of protein–DNA interactions (Jayaram *et al.*, 1991). Although the MC model qualitatively describes salt effects in the λcI repressor–operator interaction, it substantially underestimates the salt dependence of the binding free energy. In addition, MC treatments are computationally quite expensive. The NLPB model is useful not only because of its accuracy, but also because of its relatively modest computational requirements.

We report here on the application of the finite difference PB (FDPB) method to evaluate the salt dependent contribution to the total electrostatic free energy of binding of proteins to DNA. The λcI repressor–operator (Sauer *et al.*, 1990; Ptashne, 1987) and the *Eco*RI endonuclease–DNA (Rosenberg, 1991; Modrich, 1982) systems are among the most extensively studied protein–DNA complexes. An important characteristic for the function of both of these proteins is their differential binding affinity for various DNA sequences (Senear & Batey, 1991; Lesser *et al.*, 1990; Sauer *et al.*, 1990; Ptashne, 1987; Terry *et al.*, 1983; Modrich, 1982). The cocrystal structures of both the λcI repressor–O_L1 operator (Beamer & Pabo, 1992; Jordan & Pabo, 1988) and the *Eco*RI endonuclease-d[(TCG CGAATTCGCG)$_2$] (Kim *et al.*, 1990; McClarin *et al.*, 1986) complexes delineate specific hydrogen bond contacts to conserved base pairs as important determinants of DNA binding specificity. However, these direct contacts cannot account for the differential specificity of the λcI repressor for its different operator sites (Senear & Batey, 1991), nor can they fully account for the high sequence selectivity of the *Eco*RI endonuclease (Lesser *et al.*, 1990). As such, indirect effects of DNA sequence are thought to be important determinants of specificity in these systems (Senear & Batey, 1991; Lesser *et al.*, 1990).

The affinity of each of these proteins for DNA is highly dependent on salt concentration (Koblan & Ackers, 1991*a*; Senear & Batey, 1991; Nelson & Sauer, 1985; Jen-Jacobsen *et al.*, 1983; Terry *et al.*, 1983). Indeed, it has been shown that salt effects contribute significantly to the discrimination of DNA binding sites for both the λcI repressor and the *Eco*RI endonuclease (Koblan & Ackers, 1991*a*; Senear & Batey, 1991; Terry *et al.*, 1983). Thus, these are ideal systems in which to analyze the role of salt in binding.

This study focuses on the role of nonspecific univalent salt effects in the salt dependent interactions

of the λcI repressor protein and the *Eco*RI restriction endonuclease with their respective DNA fragments. A detailed physical interpretation of salt dependent electrostatic effects on protein–DNA interactions is presented. The finite difference NLPB approach provides an initial step towards a detailed atomic level understanding of the role of salt in site-specific DNA recognition.

2. Methods

(a) *Theory*

(i) *The NLPB equation*

The NLPB equation for a macromolecule in a 1:1 salt solution is:

$$\nabla\cdot[\varepsilon(\mathbf{r})\nabla\cdot\phi(\mathbf{r})]-\varepsilon\kappa^2\sinh[\phi(\mathbf{r})]+4\pi e\rho^{f}(\mathbf{r})/kT=0, \quad (1)$$

where $\phi(\mathbf{r})$ is the dimensionless electrostatic potential in units of kT/e in which k is Boltzmann's constant, T is the absolute temperature, and e is the proton charge. In addition, ε is the dielectric constant and ρ^{f} is the fixed charge density. The term $\kappa^2=1/\lambda^2=8\pi e^2 I/\varepsilon kT$, where λ is the Debye length and I is the ionic strength of the bulk solution. The quantities ϕ, ε, κ and ρ are all functions of the position vector $\mathbf{r}$ in the reference frame centered on a fixed macromolecule.

The total electrostatic free energy of a system described by the NLPB equation can be written (Sharp & Honig, 1990*a*):

$$\Delta G^{el}=\int\{\rho^{f}\phi^{f}/2+\rho^{f}\phi^{m}+\rho^{m}\phi^{m}/2-(\rho^{m}\phi+\Delta\Pi)\}\,dv, \quad (2)$$

where the potential, ϕ, and charge density, ρ, have been split up into contributions from the fixed, f, and the mobile, m, charges. The osmotic pressure term $\Delta\Pi=kTc^{b}[2\cosh(\phi)-2]$ is the excess concentration of ions at any point in solution relative to the bulk concentration of ions, c^{b}. The first term, $\Delta G^{\circ}_{ns}=\int(\rho^{f}\phi^{f}/2)\,dv$, is the total electrostatic solvation free energy of the macromolecule in pure solvent without salt. The contribution of salt to the electrostatic solvation free energy of the fixed macromolecule, ΔG°_{s}, is given by the remaining three terms in equation (2):

$$\Delta G^{\circ}_{s}=\int\{\rho^{f}\phi^{m}+\rho^{m}\phi^{m}/2-(\rho^{m}\phi+\Delta\Pi)\}\,dv. \quad (3)$$

ΔG°_{s} can be subdivided into 3 terms (Misra *et al.*, 1994): the purely entropic free energy of organizing the ion atmosphere, $\Delta G^{\circ}_{org}=\int\{-(\rho^{m}\phi+\Delta\Pi)\}\,dv$; the electrostatic self energy of charging the ion atmosphere, $\Delta G^{\circ}_{ii}=\int(\rho^{m}\phi^{m}/2)\,dv$; and the electrostatic free energy of placing the fully charged macromolecule in the fully assembled and charged ion atmosphere, $\Delta G^{\circ}_{im}=\int(\rho^{f}\phi^{m})\,dv$.

(ii) *Salt effects on binding*

The salt dependence of a protein–DNA binding reaction must by analyzed as a 2-step process:

$$D \overset{K_1}{\rightarrow} D^* \quad (4)$$

$$D^*+P \overset{K_2}{\rightarrow} D^*P, \quad (5)$$

where D is native *B*-DNA, D* is the conformation of DNA in the protein–DNA complex, P is the protein; and K_i is the association constant for each reaction. The experimentally observed association constant, K_{obs}, is obtained from the sum of reactions (4) and (5) such that:

$$K_{obs}=(K_1)(K_2). \quad (6)$$

Therefore, the total salt dependence of K_{obs} is simply:

$$\frac{\partial(\ln K_{obs})}{\partial(\ln[M^+])}=\frac{\partial(\ln K_1)}{\partial(\ln[M^+])}+\frac{\partial(\ln K_2)}{\partial(\ln[M^+])}. \quad (7)$$

From the NLPB equation, the variation in $-\ln K_{obs}$ with $\ln[M^+]$ is:

$$-\frac{\partial(\ln K_{obs})}{\partial(\ln[M^+])}=\frac{\partial(\Delta\Delta G_s)}{kT\,\partial(\ln[M^+])}=\frac{\partial(\Delta\Delta G_{s1})}{kT\,\partial(\ln[M^+])}+\frac{\partial(\Delta\Delta G_{s2})}{kT\,\partial(\ln[M^+])}, \quad (8)$$

where $\Delta\Delta G^{\circ}_{si}$ is the change in the salt dependent contribution to the total electrostatic free energy for each reaction (Misra *et al.*, 1994). The quantity $\Delta\Delta G^{\circ}_{s}$ can be partitioned into differences in ion–molecule, $\Delta\Delta G^{\circ}_{im}$; ion–ion, $\Delta\Delta G^{\circ}_{ij}$; and organizational, $\Delta\Delta G^{\circ}_{org}$ free energies. This analysis emphasizes how changes in the ion distributions around the macromolecules affect the solvation free energy upon binding.

(b) *Molecular model*

The bound and free molecules were described by the 3-dimensional structure of the protein–DNA complexes listed below. The molecule is treated as a low dielectric medium (ε_m) within the volume enclosed by the water-accessible surface of the macromolecule (probe radius = 1·4 Å). For the cases studied here, results were calculated for $\varepsilon_m=2$ and 4 (Sharp & Honig, 1990*b*; Harvey, 1988; Gilson & Honig, 1986). Two partial charge distributions were examined. Partial charges derived from both the CVFF (Hagler *et al.*, 1979) and AMBER (Weiner *et al.*, 1986) forcefield parameters were assigned to the center of each atom. The surrounding solvent was treated as a continuum of dielectric constant (ε_s) 80 with a 1:1 electrolyte distributed according to a Boltzmann weighted average of the mean electrostatic potential. A 2·0 Å ion exclusion radius (corresponding roughly to the hydrated radius of a sodium ion) was added to the surface of the macromolecules to account for ion size. Our calculations vary by less than 5% with charge set and internal dielectric constant. Results are given for the CVFF charge set and $\varepsilon_m=4$.

The refined atomic coordinates of the NH_2-terminal domain of the λcI repressor (the DNA binding domain) bound to a 20 bp oligonucleotide containing the O_L1 operator were kindly provided by Dr Carl O. Pabo (Beamer & Pabo, 1992). The first 5 amino terminal residues in the nonconsensus half-site of the λcI repressor were missing in the crystallographic structure of the complex. These residues were built as a mirror image of the consensus half-site and energy minimized with the molecular simulation program DISCOVER (Biosym, 1993). The calculated salt dependence varies by less than 5% for a group of structures which vary by about 3 Å RMSD for the modeled residues. The Glu34→Lys (EK34) λcI repressor mutant was constructed by replacing the Glu34 side chains with Lys side chains followed by energy

minimization of positions 33, 34 and 35. The calculated salt dependence varies by less than 3% for Lys34 side-chain conformations which vary by as much as 6 Å. Before assigning partial charges to each atom, protons were added to each molecule and minimized with all heavy atoms fixed to reduce van der Waals overlaps and maximize hydrogen bonds. All ionizable groups on the proteins were fully charged in the free and bound state consistent with pH titration data at neutral pH (Senear & Ackers, 1990). Proton-linked effects on the λcI repressor–O_R operator interaction are currently being analyzed (Misra & Honig, unpublished results).

The interaction of the λcI repressor monomer with each O_L1 operator half-site was modeled using the available crystallographic structure. Each monomer–half-operator complex was generated by simply removing the atoms of the opposite monomer from the complex. These complexes were used to calculate the contribution of structure dependent differences in the salt dependent interaction of the λcI repressor monomer with each half-site to the overall salt dependence of the interaction.

The refined crystallographic coordinates of the *Eco*RI endonuclease-d[(TCGCGAATTCGCG)$_2$] complex were provided by Dr John M. Rosenberg (Kim *et al.*, 1990; McClarin *et al.*, 1986). The first 15 amino terminal residues were absent in the crystallographic structure of the complex. In order to construct the wild-type (WT) *Eco*RI endonuclease, these residues were built onto the protein. Experimental evidence strongly suggests that the N terminus is required for catalytic activity (Jen–Jacobsen *et al.*, 1986). Therefore, the N terminus was positioned within about 10 Å from the phosphate group of the adenine residue at the catalytic site using the DISCOVER software package (J. Rosenberg, personal communication). N terminal deletion mutants lacking the first 4 (DELN4), 12 (DELN12) and 29 (DELN29) amino acid residues of the WT protein were also studied. The DELN4 mutant was constructed by deleting 4 residues from the WT protein described above. The DELN12 mutant was constructed by adding 3 residues in an extended (β-sheet) conformation to the N terminus of the crystallographic structure. The DELN29 mutant was constructed by deleting 14 residues from the N terminus of the crystallographic structure. Once again, protons were added to each molecule and energy minimized using DISCOVER with all heavy atoms fixed.

The *Eco*RI endonuclease protein was charged according to an initial calculation of the pK_a values of the ionizable residues in the bound complex (Hecht & Honig, unpublished results; Yang *et al.*, 1993). In the free protein, each of the basic residues was charged to −1, each of the acidic residues was charged to +1, and each histidine was neutral. Based on our initial calculations of pH dependent effects (Hecht & Honig, unpublished results), we anticipate that the pK_a of His114 will be shifted upward on binding since it is proximal to the DNA. Therefore, we have charged His114 to +1 in the bound state. This pK_a shift is consistent with the experimentally observed pH linked effects on binding (Jen-Jacobsen *et al.*, 1983).

In each case, the salt-dependence of the DNA transition from the *B*-conformation to the bound conformation was calculated. For the *Eco*RI endonuclease, the conformation of *B*-form d[(CGCGAATTCGCG)$_2$] was defined by the single-crystal X-ray diffraction structure of the oligonucleotide (Drew *et al.*, 1981). The coordinates of the *B*-DNA form of the O_L1 operator sequence was generated from the idealized local coordinates of Arnott & Hukins (1972) using the InsightII/DISCOVER modeling package (Biosym, 1992, 1993). The use of the canonical *B*-DNA conformation introduces some error into our calculations. However, the variation in the salt dependence for various forms of free *B*-DNA is relatively small (<5%). Furthermore, the salt dependent free energy is a significant but small part of the total salt dependent binding free energy, so that structural uncertainty results in only a small error in the overall salt dependence of binding. No attempt was made to explicitly account for structural changes in the protein upon binding. Since the known crystal structures of the free and bound proteins are quite similar (Beamer & Pabo, 1992; Rosenberg, 1991; Jordan & Pabo, 1988), the salt dependencies of these transitions are expected to be very small due to the relatively small local charge densities of the proteins. These effects can later be included in more sensitive analyses of binding energies.

(c) *Calculation of the electrostatic free energy*

Electrostatic potentials were calculated with the finite difference NLPB equation implemented in the DelPhi software package (Nicholls & Honig, 1991; Jayaram *et al.*, 1989; Gilson & Honig, 1988; Gilson *et al.*, 1988). The macromolecule and the surrounding solvent were mapped onto a 65^3 lattice. The largest source of error in the finite difference method arises from the limited resolution of the lattice and the resulting error in the representation of the molecular surface (Gilson *et al.*, 1988). Therefore, the potentials were calculated using a 3-step focussing technique (Gilson *et al.*, 1988). In the initial calculation, the largest dimension of the macromolecule fills 23% of the grid and the potentials at the lattice points on the boundary of the grid are approximated analytically using the Debye–Hückel equation such that $\phi(\infty) = 0$ (Klapper *et al.*, 1986). The final potentials are calculated in 2 steps in which the grid is made 4 times finer, such that the largest dimension of the macromolecule fills 92% of the grid with the boundary conditions interpolated from the previous step. The final resolution for the ligand–DNA complexes was at least 0·9 grid/Å. At this resolution, salt dependent electrostatic free energies vary by less than 1% with respect to grid placement and resolution. Each of the salt-dependent free energy terms (eqn (3)) were calculated with the appropriate numerical integrals over the lattice as previously described (Misra *et al.*, 1994).

3. Results

As shown in Table 1, the calculated values of the salt dependence for the λcI repressor–operator and *Eco*RI endonuclease–DNA systems are in excellent agreement with experiment. The calculated values of the salt dependent binding free energies, $\Delta\Delta G^\circ_s$, increase linearly with ln [M$^+$] (Figures 1 to 3). $\Delta\Delta G^\circ_s$ has been interpreted in terms of the changes in three salt dependent free energy contributions (Tables 2 to 5; Figures 2 and 3): the electrostatic ion–molecule interaction free energy, ΔG°_{im}; the electrostatic ion–ion interaction free energy upon binding, ΔG°_{ii}; and the purely entropic free energy of ion organization, ΔG°_{org} (Misra *et al.*, 1994). For each system, at physiological ionic strengths, the largest salt dependent contribution to $\Delta\Delta G^\circ_s$ and $\partial\Delta\Delta G^\circ_s/\partial \ln [M^+]$ is the large unfavorable change in the ion molecule interactions; these changes are mirrored by smaller favorable changes in ΔG°_{ii}. While long range electrostatic effects are manifested in $\Delta\Delta G^\circ_{im}$ and $\Delta\Delta G^\circ_{ii}$, the small changes in ΔG°_{org} reflect changes in the local

ion distributions upon binding. Overall, $\Delta\Delta G^{\circ}_{s}$ substantially destabilizes both the λcI repressor–operator and *Eco*RI endonuclease–DNA complexes (Tables 2 and 4). These findings are qualitatively similar to those observed in a variety of minor groove binding antibiotics (Misra *et al.*, 1994). However, here, a substantial part of the overall salt dependence is given by the contribution of the free proteins (Figures 2a and 3a).

These effects have been analyzed in terms of the individual components of $\Delta\Delta G^{\circ}_{s}$ for the free proteins, free DNA and the protein–DNA complex (Tables 2 to 5; Figures 2 and 3). The term ΔG°_{im} drives the formation of an ion atmosphere around the isolated

Table 1

Salt dependence of protein–DNA interactions

	λcI repressor		*Eco*RI endonuclease			
	WT	EK34	WT	DELN4	DELN12	DELN29
Experimental $-\partial \ln K_{obs}/\partial \ln [M^+]$	4·4 to 5·2†	7·5‡	7·4§	7·2‖	5·1‖	5·1‖
Calculated¶ $\partial\Delta\Delta G^{\circ}_{s}/\partial \ln [M^+]$	4·4	7·9	7·2	6·7	5·1	5·3

† From Senear & Batey (1991); the smaller number is from a linear least-squares regression analysis of the data, while the larger number is from a nonlinear regression analysis to account for possible competitive divalent ion effects (see the text for details).

‡ From Nelson & Sauer (1985). A linear least squares analysis of the experimental data in which the salt dependence of the repressor dimerization constant, K_d, reported by Koblan & Ackers (1991*b*) has been accounted for. In this salt range, $K_d = 3{\cdot}7$ nM; $-\partial \ln K_d/\partial \ln [M^+] = 1{\cdot}5$ (see also Senear & Batey, 1991).

§ From Jen-Jacobsen *et al.* (1983, 1986).

‖ From Jen-Jacobsen *et al.* (1986).

¶ Calculated with the finite difference NLPB equation with the CVFF charge set and $\varepsilon_m = 4$ (see the text for details). Free energy is expressed in units of kT.

Table 2

Values of salt dependent free energy terms for the λcI repressor–O_L1 operator complex at 0·1 M salt

Free energy (kcal/mol)	$B \rightarrow O_L1$†	WT‡	EK34§	Consensus‖	Nonconsensus¶
$\Delta\Delta G^{\circ}_{s}$	3·5	14·7	37·8	6·9	4·9
$\Delta\Delta G^{\circ}_{im}$	7·9	26·5	75·6	12·3	8·3
$\Delta\Delta G^{\circ}_{ii}$	−2·8	−12·1	−33·4	−5·9	−3·9
$\Delta\Delta G^{\circ}_{org}$	−1·5	0·3	−4·3	0·5	0·5

† The transition from canonical *B*-DNA to the bound form O_L1 DNA.
‡ The wild-type λcI repressor–O_L1 operator interaction.
§ The Glu34→Lys mutant λcI repressor–O_L1 operator interaction.
‖ The interaction of the repressor monomer with the consensus O_L1 operator half-site.
¶ The interaction of the repressor monomer with the nonconsensus O_L1 operator half-site.

Table 3

The salt dependence of the free energy terms for the λcI repressor–O_L1 operator complex

Free energy (kT)	$B \rightarrow O_L1$†	WT‡	EK34§	Consensus‖	Nonconsensus¶
$\partial\Delta\Delta G^{\circ}_{s}/\partial \ln [M^+]$	0·6	3·8	7·3	1·7	1·4
$\partial\Delta\Delta G^{\circ}_{im}/\partial \ln [M^+]$	0·5	7·5	12·9	3·6	3·1
$\partial\Delta\Delta G^{\circ}_{ii}/\partial \ln [M^+]$	−0·9	−4·3	−8·4	−1·9	−1·7
$\partial\Delta\Delta G^{\circ}_{org}/\partial \ln [M^+]$	1·0	0·6	2·8	0·0	0·0

† The transition from canonical *B*-DNA to the bound form O_L1 DNA.
‡ The wild-type λcI repressor–O_L1 operator interaction.
§ The Glu34→Lys mutant λcI repressor–O_L1 operator interaction.
‖ The interaction of the repressor monomer with the consensus O_L1 operator half-site.
¶ The interaction of the repressor monomer with the nonconsensus O_L1 operator half-site.

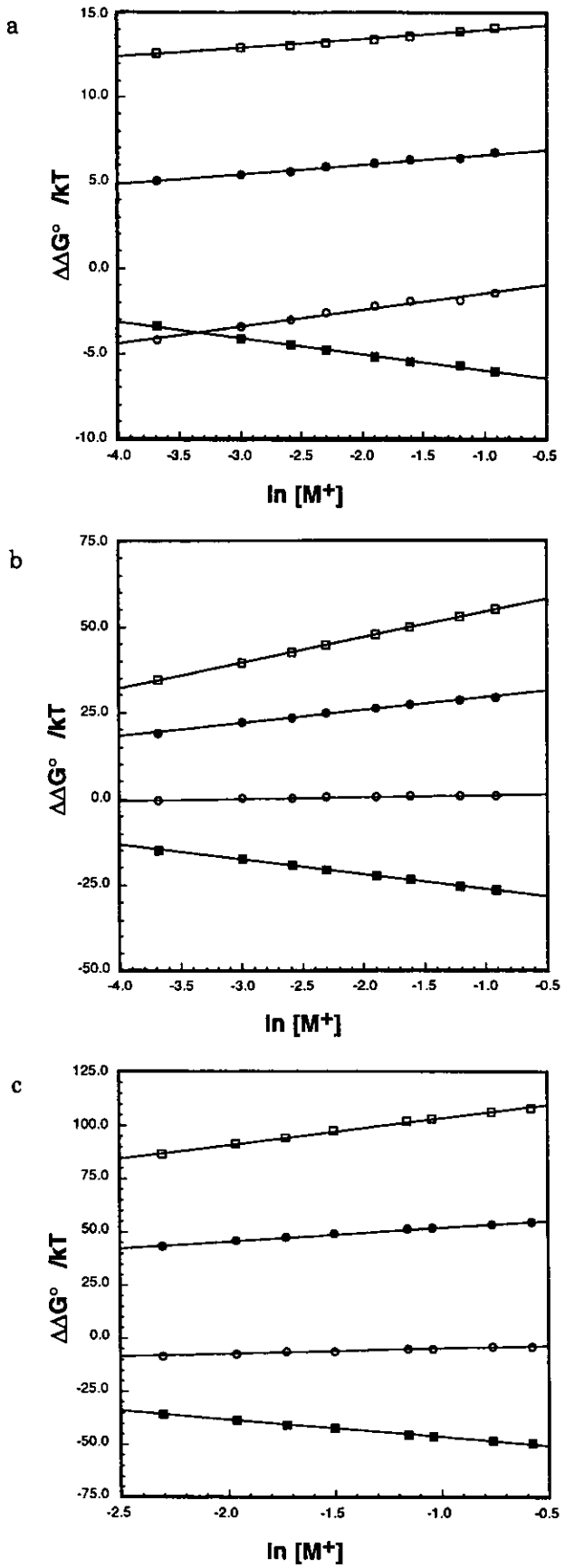

Figure 1. The calculated salt dependent contributions to the total electrostatic free energy of: a, the transition from the canonical *B* conformation to the bound conformation of the O_L1 operator sequence; b, the λ repressor-O_L1 operator interaction; and c, the *Eco*RI endonuclease-d[(CGCGAATTCGCG)$_2$] interaction. (●), $\Delta\Delta G^\circ_s$; (□), $\Delta\Delta G^\circ_{im}$; (■), $\Delta\Delta G^\circ_{ii}$; (○), $\Delta\Delta G^\circ_{org}$.

macromolecules. Cations accumulate around the DNA (Figure 4a) while anions accumulate around the DNA binding domain of the proteins (Figure 4b). Protein–DNA binding decreases the magnitude of the favorable ΔG°_{im} by dispersing the ion atmosphere around the isolated macromolecules (Tables 2 and 4; Figures 2b and 3b). This effect is caused by a redistribution of ions around both the protein and the nucleic acid upon binding (Figure 4c). The interaction of the positively charged DNA binding domain of the protein with the DNA reduces the magnitude of the negative electrostatic potential around the DNA so that fewer cations accumulate. At the same time, the large negative electrostatic potential of the DNA diminishes the anions and enriches the cations nearby the protein. In addition, the large protein molecules physically exclude cations from a high potential region near the DNA, while the DNA excludes anions from near the positively charged protein surface. The change in the ionic distribution is shown in Figure 5. The redistribution of both cations and anions upon binding decreases ΔG°_{im}. This effect increases with bulk salt concentration as proportionally more ions are displaced upon binding (Tables 3 and 5; Figures 2b and 3b).

Changes in ΔG°_{ii} also reflect the redistribution of ions upon binding. Since complex formation disperses the ion atmospheres, binding of the protein to DNA decreases ΔG°_{ii} of the system (Tables 2 and 4; Figures 2c and 3c). This effect also increases with bulk salt concentration as proportionally more ions are affected by binding (Tables 3 and 5; Figures 2c and 3c).

$\Delta\Delta G^\circ_{org}$ reveals changes in the local ion distributions. The behaviour of $\Delta\Delta G^\circ_{org}$ in protein–DNA systems is much more complicated than that seen in simple ligand–DNA complexes (Misra *et al.*, 1994) due to the complex molecular shapes. In contrast to the minor groove binding antibiotics, the binding of a protein to DNA can actually result in a more unfavorable ΔG°_{org} for the complex relative to the free DNA at physiological salt concentrations (Tables 2 and 4; Figures 2d, 3d and 6). This effect results from the entropically unfavorable accumulation of cations in solvent filled pockets with a large negative electrostatic potential at the protein–DNA interface upon complex formation (Figures 4c and 5). Since the ion distribution around the free protein also makes a significant contribution to $\Delta\Delta G^\circ_{org}$, the overall change in ΔG°_{org} may, in fact, be favorable (Tables 2 and 4; Figures 2d, 3d and 6). The magnitude of $\Delta\Delta G^\circ_{org}$ generally decreases with bulk salt concentration as the concentration difference between the local macromolecular ion atmosphere and bulk solution decreases (Tables 3 and 5; Figures 2d, 3d and 6).

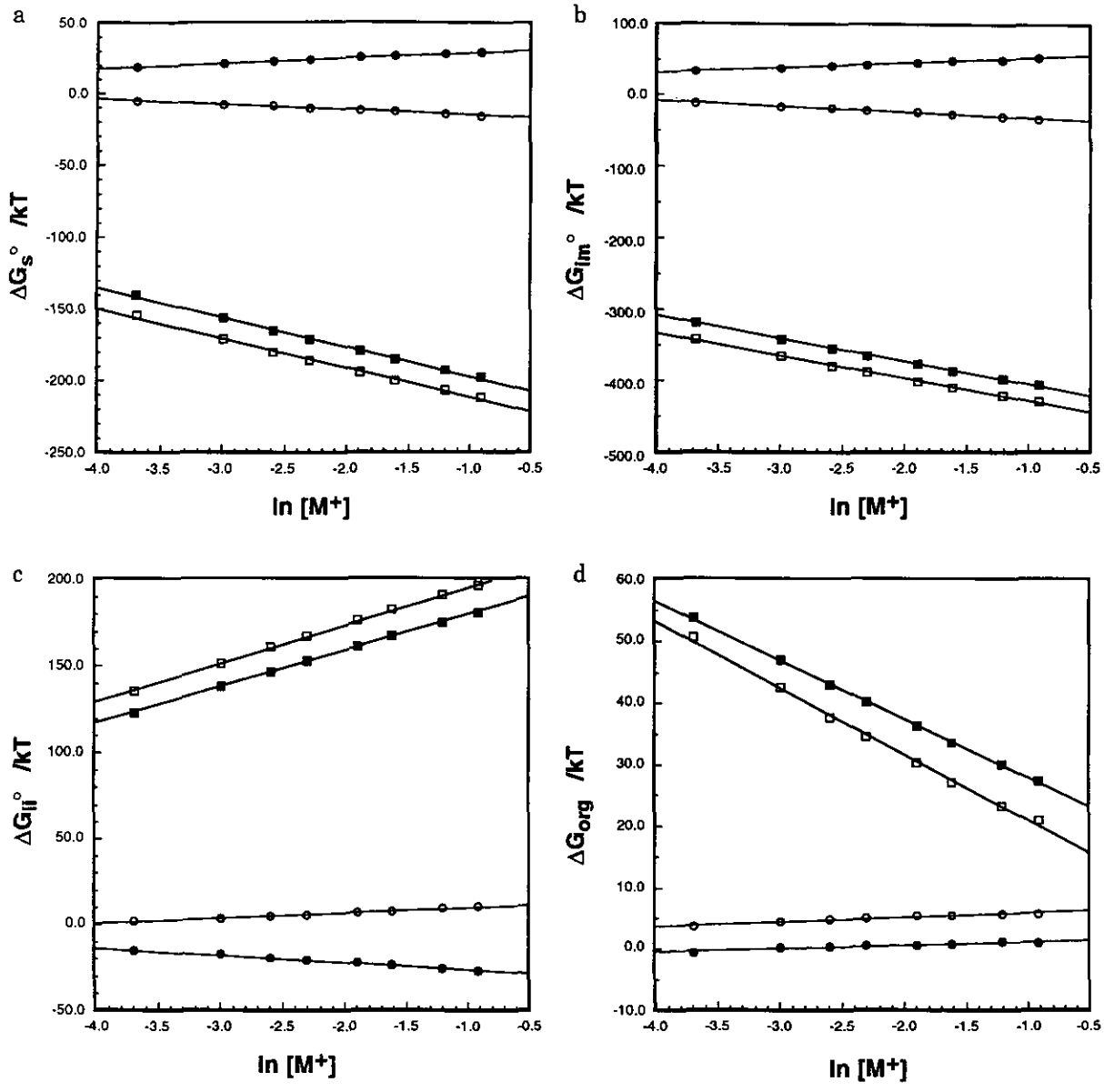

Figure 2. The salt dependent free energy terms calculated with the NLPB equation for the WT λcI repressor–O_L1 operator interaction: (■), the λcI repressor–O_L1 operator complex; (□), the bound form of the free O_L1 operator; (○), the free λcI repressor molecule; and (●), the change in the free energy calculated for the binding of the protein to the oligonucleotide. Each line represents a linear least-squares regression analysis of the data points. a, ΔG°_{s2}; b, ΔG°_{im}; c, ΔG°_{ii}; d, ΔG°_{org}.

Table 4

Values of salt dependent free energy terms for the EcoRI–*d[(CGCGAATTCGCG)$_2$] complex at 0·1 M salt*

Free energy (kcal/mol)	*B→Eco*DNA†	WT‡	DELN4§	DELN12‖	DELN29¶
$\Delta\Delta G^\circ_s$	1·4	25·6	18·2	7·9	4·8
$\Delta\Delta G^\circ_{im}$	3·4	51·3	36·5	15·0	8·5
$\Delta\Delta G^\circ_{ii}$	−1·4	−20·9	−14·5	−4·9	−1·7
$\Delta\Delta G^\circ_{org}$	−0·6	−4·8	−3·6	−2·2	−2·1

† The transition from d[(CGCGAATTCGCG)$_2$] in the free conformation (Drew *et al.*, 1981) to the bound form.

‡ The wild-type *Eco*RI–d[(CGCGAATTCGCG)$_2$] interaction.

§ The 4 amino acid N-terminal deletion mutant *Eco*RI–d[(CGCGAATTCGCG)$_2$] interaction.

‖ The 12 amino acid N-terminal deletion mutant *Eco*RI–d[(CGCGAATTCGCG)$_2$] interaction.

¶ The 29 amino acid N-terminal deletion mutant *Eco*RI–d[(CGCGAATTCGCG)$_2$] interaction.

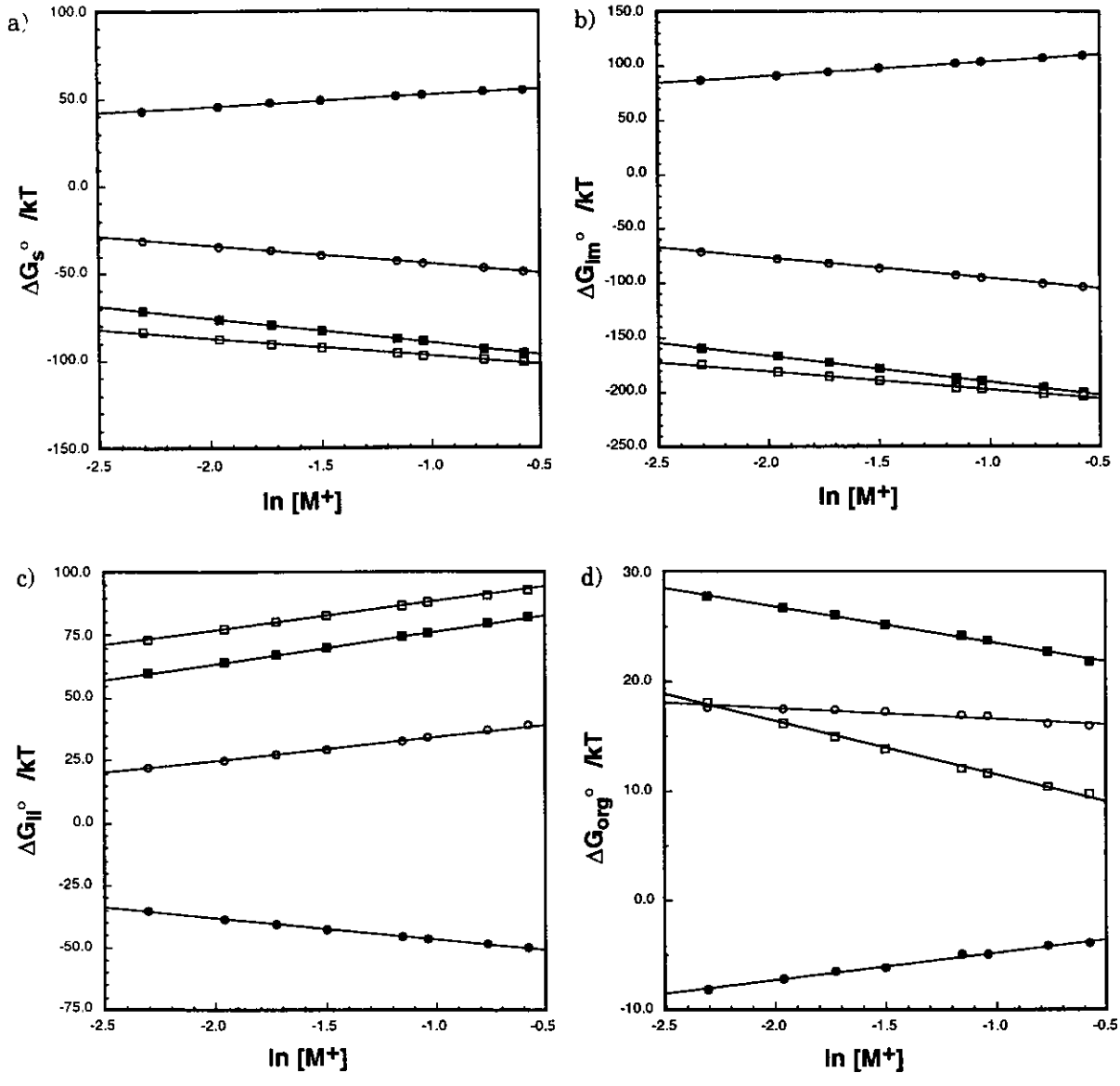

Figure 3. The salt dependent free energy terms calculated with the NLPB equation for the WT *Eco*RI endonuclease–d[(CGCGAATTCGCG)$_2$] interaction: (■), the *Eco*RI endonuclease–DNA complex; (□), the bound form of the free oligonucleotide; (○), the free *Eco*RI endonuclease; and (●), the change in the free energy calculated for the binding of the protein to the oligonucleotide. Each line represents a linear least-squares regression analysis of the data points. a, ΔG°_{s2}; b, ΔG°_{im}; c, ΔG°_{ii}; d, ΔG°_{org}.

Table 5

The salt dependence of the free energy terms for the EcoRI–d[(CGCGAATTCGCG)$_2$] complex

Free energy (kT)	$B \rightarrow$*Eco*DNA†	WT‡	DELN4§	DELN12‖	DELN29¶
$\partial\Delta\Delta G^\circ_s/\partial \ln [M^+]$	0·5	6·7	6·2	4·6	4·8
$\partial\Delta\Delta G^\circ_{im}/\partial \ln [M^+]$	0·6	12·6	11·6	9·5	9·8
$\partial\Delta\Delta G^\circ_{ii}/\partial \ln [M^+]$	−0·3	−8·4	−7·3	−5·3	−5·2
$\partial\Delta\Delta G^\circ_{org}/\partial \ln [M^+]$	0·2	2·5	1·9	0·4	0·3

† The transition from d[(CGCGAATTCGCG)$_2$] in the free conformation (Drew *et al.*, 1981) to the bound form.

‡ The wild-type *Eco*RI–d[(CGCGAATTCGCG)$_2$] interaction.

§ The 4 amino acid N-terminal deletion mutant *Eco*RI–d[(CGCGAATTCGCG)$_2$] interaction.

‖ The 12 amino acid N-terminal deletion mutant *Eco*RI–d[(CGCGAATTCGCG)$_2$] interaction.

¶ The 29 amino acid N-terminal deletion mutant *Eco*RI–d[(CGCGAATTCGCG)$_2$] interaction.

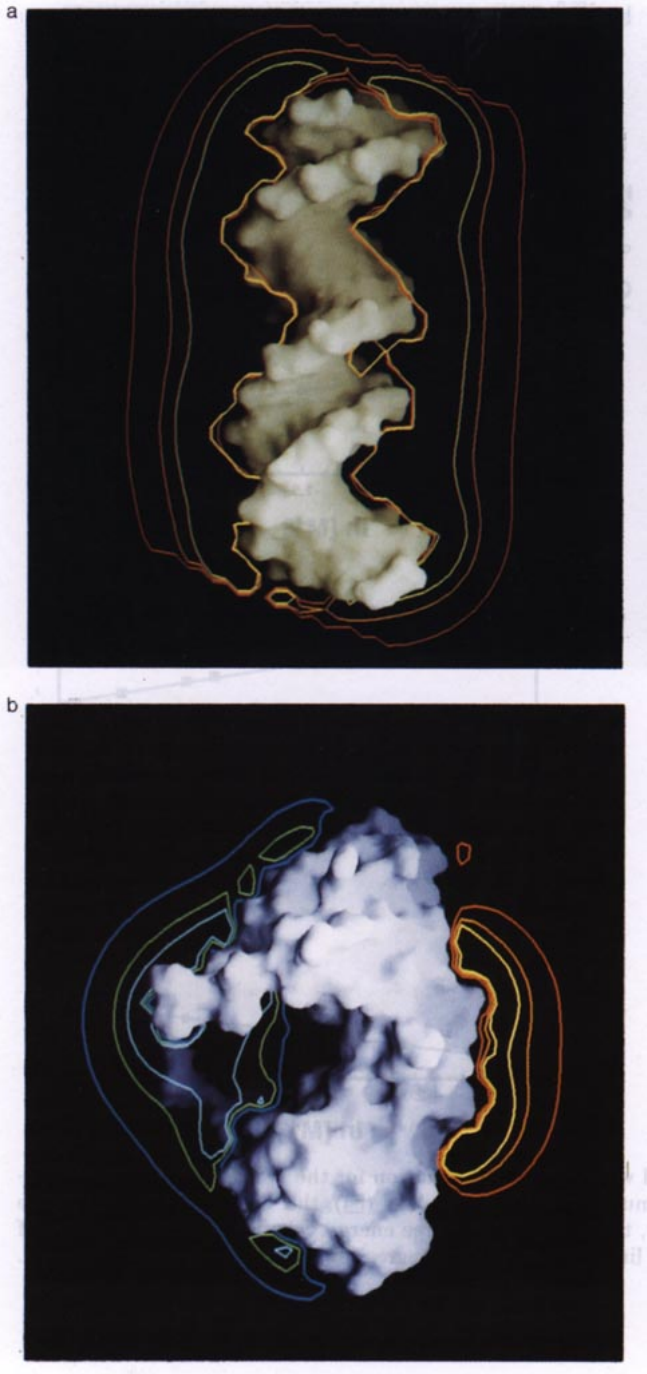

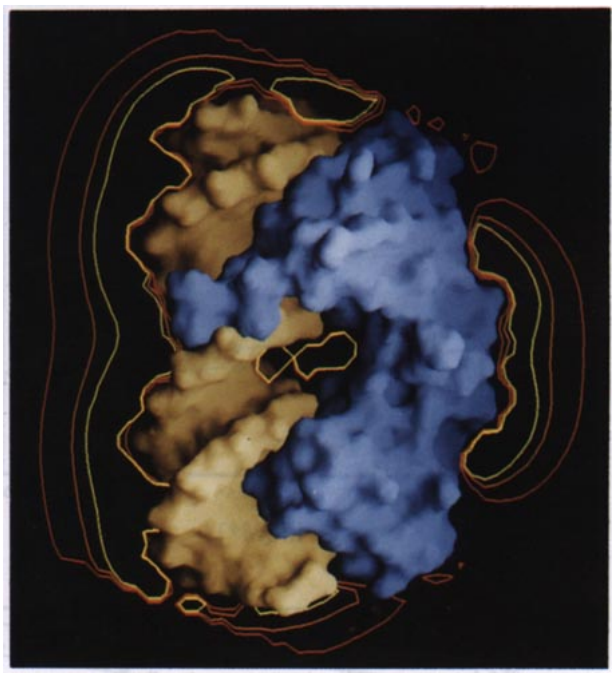

Figure 4. Two-dimensional isoconcentration univalent salt contours around the WT λcI repressor–O_L1 complex in the free and bound state at 0·1 M bulk salt concentration. Salt concentrations are given as the excess over bulk salt concentration. Excess cation distributions are shown as: red, 0·1 M; orange, 0·2 M; yellow, 0·3 M. Excess anion distributions are represented by: blue, 0·1 M; green, 0·2 M; cyan, 0·3 M. The macromolecules are represented by their solvent accessible surfaces (probe radius = 1·4 Å). a, The bound form of the free O_L1 operator; b, The free λcI repressor; c, The λcI repressor–O_L1 operator complex.

(a) *The λcI repressor–O_L1 operator complex*

(i) *The DNA structural transition*

The site specific binding of the λcI repressor to its operator results in some structural changes to the DNA site (Beamer & Pabo, 1992). Therefore, we have analyzed the salt dependence of binding according to the two-step process given in equation (8). The calculated value of $\Delta\Delta G^\circ_{s1}$ for the DNA structural transition upon binding increases linearly with $\ln[M^+]$ such that $\partial(\Delta\Delta G^\circ_{s1})/\partial(\ln[M^+])$ equals 0·5 (Figure 1). The individual components of $\Delta\Delta G^\circ_{s1}$ for the isolated DNA in the free (D) and bound (D*) conformations are given in Figure 1 and Tables 2 and 3.

In the salt range studied, the salt dependent free energy changes associated with the structural transformation of the operator upon binding are dominated by $\Delta\Delta G^\circ_{im}$ (Figure 1; Table 2). Repressor–operator complex formation results in a widening of the major groove and bending of the DNA at the binding site (Beamer & Pabo, 1992). The phosphate–phosphate distances across the major groove are increased. These conformational changes result in lower average potentials around the operator DNA relative to canonical *B*-DNA. Consequently, ΔG°_{im} for the bound conformation of the operator, D*, is smaller than in regular *B*-DNA, D. As bulk salt concentration increases, more ions accumulate around canonical *B*-DNA relative to the operator DNA, thus increasing the relative electrostatic stability of the canonical *B*-DNA at higher salts (Figure 1 and Table 3).

Concomitant changes are seen in $\Delta\Delta G^\circ_{ii}$ and $\Delta\Delta G^\circ_{org}$ (Figure 1; Tables 2 and 3). The higher concentrations of ions around canonical *B*-DNA relative to the bound form DNA, D*, results in a more unfavorable ΔG°_{ii} and ΔG°_{org} for the canonical *B*-DNA. The term $\Delta\Delta G^\circ_{ii}$ increases with bulk salt concentration since proportionally more ions

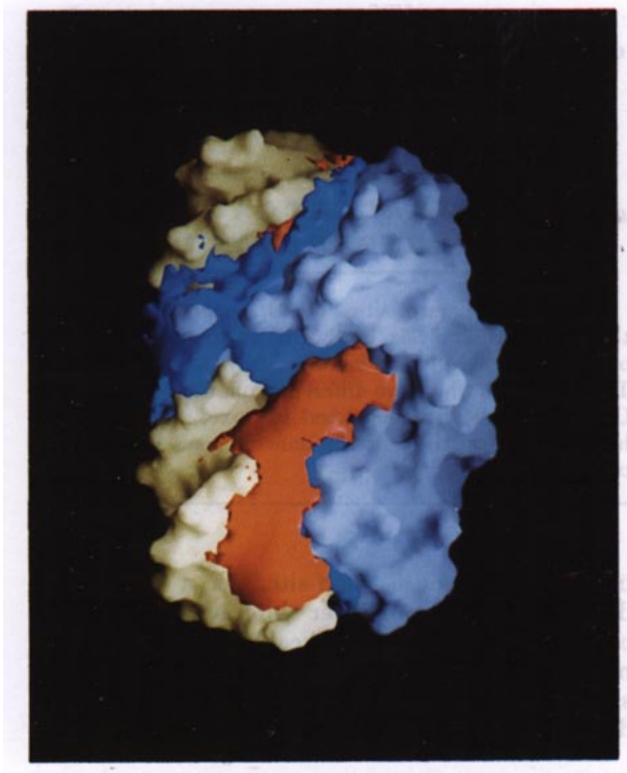

Figure 5. Three-dimensional isoconcentration contours representing the change in the net charge density around the WT λcI repressor–O_L1 operator complex upon binding. The ion concentrations around the free protein and the DNA were subtracted from the ion concentrations around the complex. The resulting salt concentrations around the complex represent the effects of nonlinearity. The red surface shows areas of accumulation of 0·62 M positive charge density (or depletion of negative charge density). The dark blue surface shows areas of depletion of 0·62 M positive charge density.

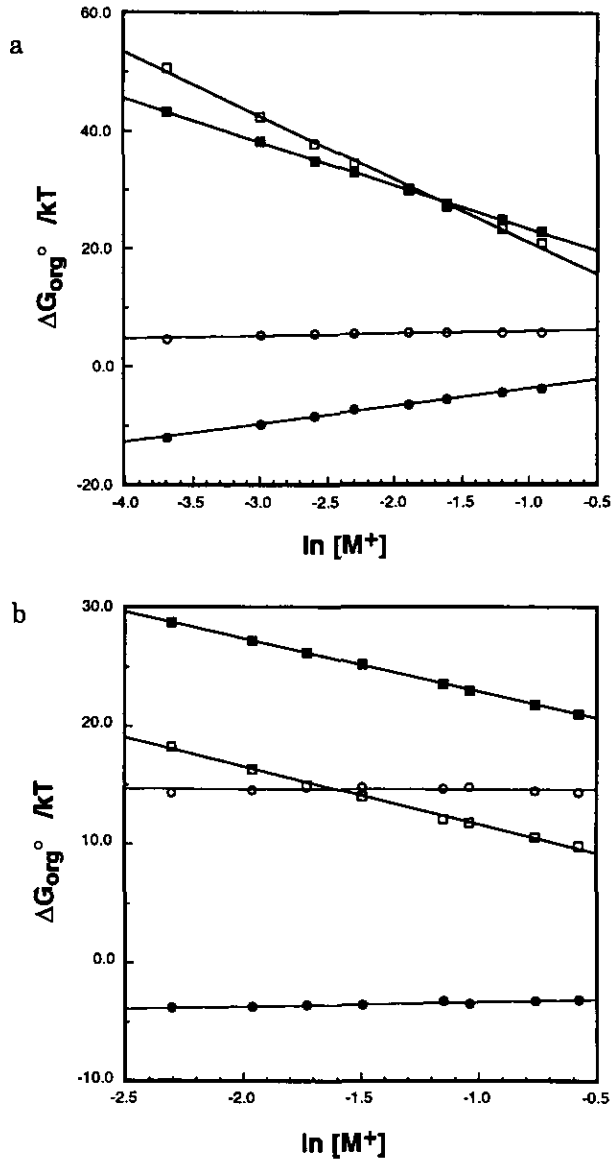

Figure 6. The salt dependence of the free energy of ion organization, ΔG°_{org}, calculated with the NLPB equation for: a, the EK34 repressor–O_L1 operator interaction; b, the DELN12 endonuclease-d[$(CGCGAATTCGCG)_2$] interaction. (■), The protein–DNA complex; (□), the bound form of the free DNA; (○), the free protein; and (●), $\Delta\Delta G^\circ_{org}$ calculated for the binding of the mutant protein to DNA. Each line represents a linear least-squares regression analysis of the data points.

accumulate around the canonical *B*-DNA relative to the operator. The unfavorable $\Delta\Delta G^\circ_{org}$ decreases with bulk salt concentration as the concentration difference between the local macromolecular ion atmosphere and bulk solution decreases.

(ii) *The wild-type (WT) λcI repressor–operator interaction*

The calculated value of $\Delta\Delta G^\circ_{s2}$ for the WT repressor dimer interaction with the operator increases linearly with ln [M^+] such that $\partial(\Delta\Delta G^\circ_{s2})/\partial(\ln [M^+])$ equals 3·8 (Figure 2a; Table 2). When the salt dependence of the DNA structural transition is added, the total salt dependence of the λcI repressor–operator interaction, $\partial(\Delta\Delta G^\circ_s)/\partial(\ln [M^+])$, is predicted to be 4·4. Overall, univalent cations are found to destabilize the λcI repressor–operator complex by more than 18 kcal/mol at 0·1 M M^+ (Table 2). It is interesting to note that $\Delta\Delta G^\circ_{org}$ actually opposes binding above about 0·05 M M^+ (Table 2; Figure 2d).

(iii) *The mutant EK34 repressor–operator interaction*

The substitution of Lys for Glu34 in the λcI repressor substantially increases the experimentally observed affinity of the protein for both operator and nonoperator sites (Nelson & Sauer, 1985). The experimentally observed value of $-\partial(\ln K_{obs})/\partial(\ln [K^+])$ of the mutant increases by about 3 relative to the WT protein (Nelson & Sauer, 1985). The calculated value of $\partial(\Delta\Delta G^\circ_s)/\partial(\ln [M^+])$ for the Glu34→Lys (EK34) repressor mutant is equal to 7·9 (Tables 1 and 3). The calculated change in $\partial(\Delta\Delta G^\circ_s)/\partial(\ln [K^+])$ upon mutation is, therefore, 3·5 relative

to the WT protein. This value agrees with the experiment very well. Salt is found to oppose the formation of the protein–DNA complex by more than 40 kcal/mol at 0·1 M M^+ (Table 2).

The major effect of the mutation is to increase the magnitude of all the contributions to both $\Delta\Delta G^\circ_{s2}$ and $\partial(\Delta\Delta G^\circ_{s2})/\partial(\ln[M^+])$ relative to the WT repressor (Tables 2 and 3). These effects are larger than those seen in the WT repressor since the more positive mutant protein interacts more unfavorably with the cationic counterion atmosphere around the DNA, while the DNA interacts more unfavorably with the more anionic ion atmosphere around the mutant protein. As a result, binding of the EK34 to its operator results in a more dispersed ion atmosphere than in the WT complex.

The role of ion redistribution is reflected in the behavior of ΔG°_{org} for the free and bound macromolecules (Figure 6). Replacing the negatively charged Glu34 side-chain with a positive lysine decreases the negative electrostatic potential at the protein–DNA interface. As a result, fewer cationic counterions accumulate in the interfacial solvent-filled pockets at each salt concentration. Therefore, an increase in ΔG°_{org} relative to the isolated DNA is only observed at high salt concentrations. The free energy associated with organizing an ion atmosphere around the free repressor dimer ensures that $\Delta\Delta G^\circ_{org}$ is always favorable (Table 2; Figure 6).

(iv) *The WT λcI repressor half-site interactions*

We have analyzed the role of salt dependent electrostatic effects in the interaction of the λcI repressor monomer with each O_L1 operator half-site. The O_L1 operator site contains an axis of approximate 2-fold symmetry and is described in terms of two half-sites (Figure 7: Sauer *et al.*, 1990; Ptashne, 1987). Each λ repressor monomer interacts with a single operator half-site. Although the λcI repressor–O_L1 operator cocrystal structure reveals that the protein dimer maintains the same specific hydrogen bond contacts to each operator half-site, the λ repressor dimer recognizes the approximately 2-fold symmetric half-operator sequences asymmetrically in terms of structure (Beamer & Pabo, 1992; Jordan & Pabo, 1988) and energetics (Sarai & Takeda, 1989). The base pair substitution experiments of Sarai & Takeda (1989) indicate that relatively small differences in the geometry of the surface of the protein with respect to the surface of the DNA revealed in the crystal structure of the two half operators result in "amazingly large" differences in binding specificity to the two half-sites. These findings indicate that indirect contacts must play a significant role in determining the specificity of the λcI repressor–operator interaction.

We find that the different salt effects in the two half-sites are a result of differences in long range electrostatic interactions, primarily in $\Delta\Delta G^\circ_{im}$ and secondarily in $\Delta\Delta G^\circ_{ii}$ (Table 2). Because of the subtle differences in the geometry of the complexes, the monomer in the consensus half-site perturbs the ion atmosphere to a greater extent than the monomer

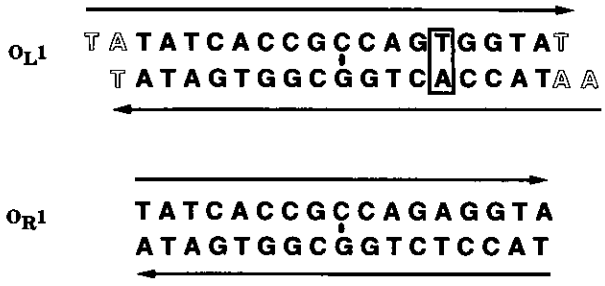

Figure 7. λ operator sites. The O_L1 operator site used in the cocrystal analysis is shown at the top. The O_R1 operator site used in the binding assays is on the bottom. The base pairs which are different from those found in the O_R1 operator site are enclosed in boxes. The consensus half-sites are on the left; the nonconsensus half-sites are on the right.

in the nonconsensus half-site. As a result, salt destabilizes the monomer interaction with the consensus half-site by 2·0 kcal/mol more than the nonconsensus half-site. These effects also result in small but significant differences in the salt dependence of binding to each half-site (Table 3).

(b) *The* Eco*RI-d[(TCGCGAATTCGCG)$_2$] complex*

(i) *The DNA structural transition*

The DNA in the *Eco*RI endonuclease complex deviates substantially from the *B*-conformation (McClarin *et al.*, 1986). The DNA in the recognition complex is kinked and unwound, resulting in a widening of the major groove to accommodate the protein. The salt dependent free energies of these structural changes are similar to those seen for the operator transition in the λ repressor–O_L1 operator complex (Tables 4 and 5). The calculated value of $\Delta\Delta G^\circ_{s1}$ for the DNA structural transition upon binding increases linearly with $\ln[M^+]$ such that $\partial(\Delta\Delta G^\circ_{s1})/\partial(\ln[M^+])$ equals 0·5 (Table 5). These free energies were explicitly included in our evaluation of the overall salt dependence of binding according to equation (8).

(ii) *The WT* Eco*RI–DNA interaction*

The salt dependence of the electrostatic effects for the binding of the *Eco*RI endonuclease to d[(CGCGAATTCGCG)$_2$], $\partial[\Delta\Delta G^\circ_s)/\partial(\ln[M^+])$, calculated with the NLPB equation equals 7·1 (Tables 1 and 5). This value agrees quite well with the experimental slope of about 7·4 determined for the binding of the *Eco*RI endonuclease to d[(CGCGAATTCGCG)$_2$] (Jen-Jacobsen *et al.*, 1983, 1986). Similar experimental results have been found for the interaction of the *Eco*RI endonuclease with plasmid DNA (Wright *et al.*, 1989; Terry *et al.*, 1983). Salt destabilizes the *Eco*RI endonuclease-d[(CGCGAATTCGCG)$_2$] complex by almost 27 kcal/mol at 0·1 M M^+ (Table 3).

(iii) Eco*RI endonuclease N-terminal deletion mutants*

We have investigated the effect of the N-terminal "arms" of the *Eco*RI endonuclease on the salt dependence of the interaction. The N-terminal arms are not required for sequence specific recognition; however, they are postulated to contribute to the stability of the complex through nonspecific electrostatic interactions with the DNA (Jen-Jacobsen *et al.*, 1986). We have calculated the salt dependent electrostatic behavior of *Eco*RI endonuclease deletion mutants lacking the first four (DELN4), 12 (DELN12) and 29 (DELN29) amino acid residues of the N-terminal arms (Jen-Jacobsen *et al.*, 1986). The calculated values of $\partial(\Delta\Delta G_s^\circ)/\partial(\ln[M^+])$ for DELN4, DELN12 and DELN29 are 6·7, 5·1 and 5·3, respectively (Tables 1 and 5). These values are in excellent agreement with the experimentally observed values of $-\partial(\ln K_{obs})/\partial(\ln[Na^+])$, found to be 7·2, 5·1 and 5·1, respectively (Jen-Jacobsen *et al.*, 1986). In each case, salt substantially destabilizes the binding of the N-terminal deletion mutants to DNA at 0·1 M M^+ (Table 5).

For each mutant, the deletion of the amino-terminal residues decreases the net charge of the protein. The deletion of the first four, 12 and 29 amino-terminal residues decreases the net charge of the protein by two, four and six relative to the WT endonuclease, respectively. These changes reduce each of the contributions to $\Delta\Delta G_{s2}^\circ$ and $\partial(\Delta\Delta G_{s2}^\circ)/\partial(\ln[M^+])$ since the less positively charged proteins now interact less unfavorably with the cationic counterion atmosphere of the DNA, while the DNA interacts less unfavorably with the more cationic ion atmosphere around the proteins. Binding of the deletion mutants to DNA thus results in less dispersal of the ion atmospheres relative to the WT protein. This effect is analogous to that observed for the EK34 λ repressor mutant and is reflected in a representative plot of ΔG_{org}° *versus* $\ln[M^+]$ (Figure 6b).

4. Discussion

(a) *The interpretation of salt effects on protein–DNA interactions in the NLPB model*

The finite difference PB model provides an accurate theoretical framework for understanding nonspecific salt dependent effects in protein–DNA systems. PB theory describes the interaction of a continuously distributed ion atmosphere with each macromolecule. The redistribution of ions upon binding reflects both differential cation and anion interactions with the protein and the DNA. As a consequence of the complicated three-dimensional shape and charge distribution, these interactions involve the accumulation and depletion of both cations and anions in specific regions around the macromolecules. The consequences of this ionic redistribution are dominated by the large unfavorable change in electrostatic ion–molecule interactions, $\Delta\Delta G_{im}^\circ$. At physiological salt concentrations, ligand binding to DNA disrupts the large favorable electrostatic interactions of the highly organized ion atmosphere with the free polyion. Although the resulting $\Delta\Delta G_{ii}^\circ$ and $\Delta\Delta G_{org}^\circ$ favor binding, they are relatively small. The resulting unfavorable change in $\Delta\Delta G_s^\circ$ upon binding indicates that the molecules are better solvated by salt in the separated state than in the bound state.

The magnitude of the salt effects calculated with the NLPB equation for the protein variants, EK34, DELN4, DELN12 and DELN29, suggests that the free energy of global salt redistribution upon binding is more important than free energy changes associated with local protein–DNA interactions (ion-pairs) in determining salt effects in ligand–DNA systems. In the WT λcI repressor–operator system, side-chain oxygen atoms of Glu34 are positioned at least 5 Å from the nearest phosphate oxygen in each half-site; the side-chain amino protons of the corresponding lysine residues in the EK34 repressor–operator system are also at least 6 Å from the nearest phosphate oxygen in each half-site. Although these residues do not make direct contacts with the DNA, the Glu34→Lys mutation increases $-\partial(\ln K_{obs})/\partial(\ln[Na^+])$ by at least three units. Similarly, in our model, the N-terminal arm of the *Eco*RI endonuclease does not make any direct contacts with the DNA, yet deletion of the first four, 12 and 29 amino acid residues decreases $-\partial(\ln K_{obs})/\partial(\ln[Na^+])$ by one to two units (Table 1). The observed changes in $-\partial(\ln K_{obs})/\partial(\ln[Na^+])$ result from changes in the ion distribution described by the NLPB equation near the protein–DNA complexes upon mutation, not ion-pairing. These changes are manifested primarily in long range electrostatic ion–molecule, $\Delta\Delta G_{im}^\circ$, and ion–ion, $\Delta\Delta G_{ii}^\circ$, interactions and secondarily in the entropy of ion organization, $\Delta\Delta G_{org}^\circ$.

The univalent salt dependence of protein–DNA binding can be a function of several other important effects: differential cation and anion binding to specific sites both on the protein and the DNA, differential protonation and differential hydration (Record *et al.*, 1978, 1991). Because of the continuum representation of salt effects in the PB model, our analysis must assume that specific ion effects, if they are present, do not substantially alter the salt dependence of binding in each of the systems studied. The results of our analyses show that salt effects in the systems studied can be accurately described in terms of simple nonspecific effects in the context of NLPB theory. Differential protonation effects can also explicitly be modeled in terms of the charge state of the protein in the free and bound states (Yang *et al.*, 1993; Misra & Honig, unpublished results; Hecht & Honig, unpublished results.

(b) *The λcI repressor–operator interaction*

The calculated salt dependence of the λcI repressor–operator interaction seems to agree quite

well with the experimental results for both the WT and EK34 proteins (Table 1). However, a simple comparison of the calculated and experimental results is complicated by a number of theoretical and experimental difficulties. These problems are discussed below.

(i) *The effect of divalent cations on the binding constant*

Our current analysis has focussed on only simple univalent ion effects. However, the repressor binding assays typically contain millimolar concentrations of divalent cations. In order to properly treat univalent salt effects, the role of divalent cations must be evaluated. Experimentally, it has been observed that low concentrations of divalent cations increase the value of $\ln K_{obs}$ for the λcI repressor–O_R operator system (Sauer *et al.*, 1990 and references cited therein). Divalent cations are thought to specifically stabilize the repressor dimer interaction with the operator (Sauer *et al.*, 1990). These effects are quite different from those observed in the nonspecific interaction of oligolysines (Lohman *et al.*, 1980) and *lac* repressor (Record *et al.*, 1977) to DNA where the addition of Mg^{2+} actually decreases the binding of the ligand.

It is important to realize that Mg^{2+} effects on binding cannot be simply described by a simple screening parameter, κ, in the NLPB model. The contribution of divalent ions to the free energy of polyelectrolyte systems has not been evaluated with an expression for the total electrostatic free energy using the NLPB equation. This is an area of current investigation. It is encouraging to note that the PB equation provides a reasonable estimate for the concentration of Mg^{2+} around highly charged cylinders in mixed NaCl–$MgCl_2$ systems relative to Monte Carlo and hypernetted chain calculations (Murthy *et al.*, 1985). Furthermore, it has been shown that competitive effects between Na^+ and Mg^{2+} in highly charged cylindrical systems can be accurately described by the NLPB equation (Wilson *et al.*, 1980). The energetic consequences of these effects on ligand–DNA interactions remain to be determined.

In the absence of a self-consistent PB approach, we have tried to extract the effect of simple 1:1 salt from the available experimental data using a very simple model which assumes that the effects of magnesium on the univalent salt dependence are negligible. In this case, the deviation in the experimental data from a simple linear model relating $-\ln K_{obs}$ to $\ln[M^+]$ was assessed. A linear least-squares regression analysis of the quantitative DNase I footprint titration data (Senear & Batey, 1991) yields a slope of 4·4(±0·4) (Table 1) with a correlation coefficient of 0·987. An analysis of the residuals for these data does not reveal any systematic deviation from the regression line that would be consistent with simple curvature due to divalent ions (Cox & Snell, 1968). Thus, despite the complicated interactions of divalent cations with the λcI repressor–O_R operator complex, these linear regression analyses provide a simple model indicating almost 98% of the variance in $-\ln K_{obs}$ can be explained by the variation in the independent variable $\ln[M^+]$.

We have also tried to account for Mg^{2+} effects using other available theoretical models. A frequently used model of divalent ion effects on ligand–nucleic acid interactions assumes that divalent cations directly compete with repressor for binding sites on the DNA (Record *et al.*, 1977). This competition is described by the following equation:

$$\log K_{obs} = \log K^\circ + m'\psi \log[M^+] + m'\log\{0{\cdot}5(1+(1+4K_{Mg,obsd}[Mg^{2+}])^{1/2})\}, \quad (9)$$

where K_{obs} is the experimentally observed association constant for the binding of repressor to DNA. Equation (9) is valid for low protein binding density in the absence of anion effects at constant pH. The first two terms on the right describe the effect of monovalent cations in the absence of Mg^{2+}; K° is the reference state thermodynamic association constant for the repressor with DNA and m' and ψ are as previously described. The last expression on the right-hand side of equation (9) is a nonlinear interaction term between the independent variables $[M^+]$ and $[Mg^{2+}]$; $K_{Mg,obsd}$ is the observed association constant for the binding of Mg^{2+} to a DNA site given by:

$$\log K_{Mg,obsd} = \log K^\circ_{Mg} - 2\psi \log[M^+]. \quad (10)$$

Although this model successfully describes the Mg^{2+} induced curvature of the $-\ln K_{obs}$ *versus* $\ln[M^+]$ plot for the nonspecific binding of *lac* repressor to DNA (Record *et al.*, 1977), the λcI repressor–O_R operator system does not behave according to a simple competitive binding model. This model predicts that the presence of divalent cations in the assay buffer results in decreased values of $\ln K_{obs}$, particularly at low univalent cation concentrations. This is contradicted by the available experimental evidence. These results might suggest that the competitive effects of divalent ions may be less important in specific protein–DNA interactions.

Nevertheless, in order to estimate the magnitude of a purely competitive divalent ion effect, we have analyzed the quantitative DNase I footprint titration data on the λcI repressor–O_R1 operator complex (Senear & Batey, 1991) with the competitive binding model using a nonlinear least-squares regression analysis. The experimental data were fitted to equation (9) with three adjustable parameters, $\log K_0$, m' and $\log K_0^M$, using a multivariate secant algorithm based on the Gauss–Newton method (SAS Institute, 1988; Ralston & Jennrich, 1978). The results of this analysis yield a value of 5·2 (95% confidence limits 4·3 to 6·0) for $-\partial(\ln K_{obs})/\partial(\ln[M^+])$ (Table 1). As a result of the overall linearity of the data points, the introduction of a curved model reduces the quality of the fit to the parameter m' relative to the simple linear model. Therefore, the results of the competitive binding

model are not statistically different from the linear model as reflected in the confidence limits of $-\partial([\ln K_{obs})/\partial[M^+])$. Presently, we cannot dismiss the possibility that divalent cations may change the slope of the regression line without substantial curvature. In either case, the NLPB model provides a reasonable estimate of $-\partial(\ln K_{obs})/\partial(\ln [M^+])$ (Table 1).

(ii) *The effect of the C-terminal domain on the binding constant*

The finite-difference NLPB calculations described here were performed on the cocrystal structure of the N-terminal (DNA binding) domain (residues 1 to 92) of the λcI repressor bound to the O_L1 operator site (Beamer & Pabo, 1992), whereas the corresponding experimental studies (Koblan & Ackers, 1991*a*; Senear & Batey, 1991; Nelson & Sauer, 1985) were performed on the intact repressor protein. The intact repressor is known to bind operator DNA 100 to 1000-fold more tightly than the N-terminal domain alone (Sauer *et al.*, 1990 and references cited therein). However, this difference arises mainly because the intact repressor forms a more stable dimer (Sauer *et al.*, 1990). Thus, the value of the observed dissociation constant, K_{obs}, for the interaction of the intact repressor dimer and the N-terminal dimer with their operators are the same to within experimental error (Sauer *et al.*, 1990). From these data, it seems that preformed dimers of both species bind the operator with approximately equal affinity. The NLPB calculations involve only K_{obs}.

The effect of the C-terminal domain (residues 93 to 236) on the salt-dependence of K_{obs} are likely to be small as well. This domain is made up of two independently folding regions (Pabo *et al.*, 1979) attached to the N-terminal domain more than 27 Å from the DNA (Beamer & Pabo, 1992). Furthermore, the pattern of protection from chemical methylation and DNase I cleavage observed for the intact repressor and the N-terminal domain are identical (Sauer *et al.*, 1990), indicating that the C-terminal domain does not contact the DNA. It is anticipated that charged groups more than about 10 to 15 Å from the DNA will have little effect on the salt-dependence of K_{obs}. However, in the absence of detailed structural information, these caveats must be kept in mind.

(iii) *The effect of the operator sequence on the binding constant*

Site-specific variation of salt effects may complicate the direct comparison of our calculations with experimental data. Our calculations were performed on the λcI repressor bound to the O_L1 operator sequence (Beamer & Pabo, 1992), while the corresponding experimental studies were done on the O_R1 operator sequence (Koblan & Ackers, 1991*a*; Senear & Batey, 1991; Nelson & Sauer, 1985). However, the variation in the salt dependence between the O_R1 and O_L1 sites is expected to be small. The O_L1 site differs from the O_R1 site at only a single noncontacted base pair (Figure 7); the resulting change in the binding free energy change is negligible (Sarai & Takeda, 1989). This implies that the structure of the two complexes should be quite similar. Given these data, it is reasonable to assume that the salt dependencies of repressor binding to the O_R1 and O_L1 sites are comparable.

(c) *The* Eco*RI endonuclease–DNA interaction*

The calculated salt dependencies of the interaction of both the WT and mutant *Eco*RI endonucleases with d[$(CGCGAATTCGCG)_2$] agree extremely well with the experimental results (Table 1). The experimental salt dependencies were determined for the binding of the endonuclease to d[$(CGCGAATTCGCG)_2$] using a filter binding assay without added Mg^{2+} (Jen-Jacobsen *et al.*, 1983, 1986). Identical results have been found for the interaction of the endonuclease with plasmid DNA in the absence of Mg^{2+} (Wright *et al.*, 1989; Terry *et al.*, 1983). As such, a direct comparison of the calculated and experimental results is relatively straightforward above 0·1 M $[M^+]$.

The interpretation of the experimental results is complicated for salt concentrations below 0·1 M Na^+. In the low salt region, the graph of $-\ln K_{obs}$ *versus* $\ln [Na^+]$ significantly deviates from linearity in the absence of divalent ions (Jen-Jacobsen *et al.*, 1983; Terry *et al.*, 1983). In fact, $-\partial(\ln K_{obs})/\partial(\ln [Na^+])$ actually becomes positive indicating that binding is enhanced by increasing salt concentrations. A similar phenomenon has been observed in a variety of protein–DNA systems including the *lac* repressor–operator system (Winter & von Hippel, 1981), the catabolite gene activator protein (CAP)–DNA system (Ebright *et al.*, 1989), the P22 *mnt* repressor–operator system (Vershon *et al.*, 1987*a*), the P22 *arc* repressor–operator system (Vershon *et al.*, 1987*b*), and the AraC protein–DNA interaction (Martin & Schleif, 1987). Part of this effect may be explained by aggregation of the protein at low ionic strength (Jen-Jacobsen *et al.*, 1983) or, possibly, conformational changes in the protein upon binding (Martin & Schleif, 1987). It has also been suggested that nonlinearity is due to differential anion binding, differential cation binding, and differential ion screening (Record *et al.*, 1978, 1991). However, the extent to which the observed curvature represents differential cation and anion binding unexplained by the NLPB equation is uncertain. A careful evaluation of salt effects in the low salt region is being conducted.

(d) *The role of salt effects on the specificity of protein–DNA interactions in the NLPB model*

It has been observed that the magnitude of the salt dependence of repressor binding varies among the O_R operator sites (Koblan & Ackers, 1991*a*; Senear & Batey, 1991). These data indicate that salt dependent effects can play a significant role in the overall free energy differences found for site specific

binding. The finite-difference PB analysis presented here emphasizes the importance of three-dimensional structure in describing the salt dependence of protein–DNA interactions. The role of geometry in determining the specificity of protein binding to DNA is not limited to the number of direct hydrophobic, hydrogen bond and ion-pair contacts; rather, geometry also plays a role in determining the interaction free energy of the molecule with solvent and ions. In the NLPB model, differences in the shape and charge distribution of macromolecules lead to changes in their ion distributions which results in changes in the ion interaction free energy with the macromolecules.

The role of salt effects in site-specific recognition is evident from the analysis of the λcI repressor–half operator interaction. Subtle differences in the geometry of the two complexes lead to a salt dependent contribution to the free energy of binding to the consensus half-site which is 40% more unfavorable than the salt dependent contribution to the free energy of binding to the nonconsensus half-site at 0·1 M salt (Table 2). In addition, the salt dependence of binding to the two half-sites differs by almost 20% (Table 3). It is possible that these types of differences may be responsible for the different salt effects observed among the O_R operator sites (Koblan & Ackers, 1991*a*; Senear & Batey, 1991). Concomitant structure dependent changes in the essentially salt independent hydrophobic, hydrogen-bond and ion-pair contacts must also contribute to differences in the binding free energy; however, quantitative estimates of these contributions remain to be determined.

We thank Drs Timothy Lohman, Donald Senear and Martin Zacharias for helpful discussions and correspondence. We also thank Dr Dawn P. Misra for help with statistical analyses and Drs Carl O. Pabo and John M. Rosenberg for providing crystallographic coordinates. This work was supported by NIH grant no. GM-41371 and NSF grant no. MCO-92-20477.

References

Alfrey, T. J., Berg, P. W. & Morawetz, H. (1951). The counterion distribution in solutions of rod-shaped electrolytes. *J. Polymer Sci.* **7**, 543–547.

Anderson, C. F. & Record, M. T. (1982). Polyelectrolyte theories and their applications to DNA. *Annu. Rev. Phys. Chem.* **33**, 191–222.

Anderson, C. F. & Record, M. T. (1983). The thermodynamic effects of polyelectrolyte–electrolyte interactions. In *Structure and Dynamics: Nucleic Acids and Proteins* (Clementi, E. & Ramaswamy, H. S., eds), pp. 301–318, Adenine Press, New York.

Anderson, C. F. & Record, M. T. (1990). Ion distributions around DNA and other cylindrical polyions: theoretical descriptions and physical implications. *Annu. Rev. Biophys. Chem.* **19**, 423–465.

Arnott, C. F. & Hukins, D. W. (1972). Optimised parameters for *A*-DNA and *B*-DNA. *Biochem. Biophys. Res. Commun.* **47**, 1504–1509.

Beamer, L. J. & Pabo, C. O. (1992). Refined 1·8 Å crystal structure of the λ repressor–operator complex. *J. Mol. Biol.* **227**, 177–196.

Biosym (1992). InsightII 2.2.0. Biosym Technologies, Inc., San Diego.

Biosym (1993). DISCOVER 3.1. Biosym Technologies, Inc., San Diego.

Cox, D. R. & Snell, E. J. (1968). A general definition of residuals. *J. R. Statist. Soc. B*, **30**, 248–275.

deHaseth, P. L., Lohman, T. M. & Record, M. T. (1977). Nonspecific interaction of *lac* repressor with DNA: an association reaction driven by counterion release. *Biochemistry*, **16**, 4783–4790.

Drew, H. R., Wing, R. M., Takano, T., Broka, C., Tanaka, S., Itakura, K. & Dickerson, R. E. (1981). Structure of a *B*-DNA dodecamer: conformation and dynamics. *Proc. Nat. Acad. Sci., U.S.A.* **78**, 2179–2183.

Ebright, R. H., Ebright, Y. W. & Gunasekera, A. (1989). Consensus DNA site for the *Escherichia coli* catabolite gene activator protein (CAP): CAP exhibits a 450-fold higher affinity for the consensus DNA site than for the *E. coli lac* DNA site. *Nucl. Acids Res.* **17**, 10295–10305.

Fuoss, R. M., Katchalsky, A. & Lifson, S. (1951). The potential of an infinite rod-like molecule and the distribution of counter ions. *Proc. Nat. Acad. Sci., U.S.A.* **37**, 579–589.

Gilson, M. K. & Honig, B. H. (1986). The dielectric constant of a folded protein. *Biopolymers*, **25**, 2097–2119.

Gilson, M. K. & Honig, B. (1988). Calculation of the total electrostatic energy of a macromolecular system: solvation energies, binding energies, and conformational analysis. *Proteins: Struct. Funct. Genet.* **4**, 7–18.

Gilson, M. K., Sharp, K. A. & Honig, B. H. (1988). Calculating the electrostatic potential of molecules in solution: method and error assessment. *J. Comput. Chem.* **9**, 327–335.

Hagler, A. T., Stern, P. S., Sharon, R., Becker, J. M. & Naider, F. (1979). Computer simulation of the conformational properties of oligopeptides. Comparison of theoretical methods and analysis of experimental results. *J. Amer. Chem. Soc.* **101**, 6842–6852.

Harrison, S. C. & Aggarwal, A. K. (1990). DNA recognition by proteins with the helix-turn-helix motif. *Annu. Rev. Biochem.* **59**, 933–969.

Harvey, S. (1988). Treatment of electrostatic effects in macromolecular modeling. *Proteins: Struct. Funct. Genet.* **5**, 78–92.

Honig, B., Sharp, K. & Yang, A. (1993). Macroscopic models of aqueous solutions: biological and chemical application. *J. Phys. Chem.* **97**, 1101–1109.

Jayaram, B., Sharp, K. A. & Honig, B. (1989). The electrostatic potential of DNA. *Biopolymers*, **28**, 975–993.

Jayaram, B., DiCapua, F. M. & Beveridge, D. L. (1991). A theoretical study of polyelectrolyte effects in protein–DNA interactions: Monte Carlo free energy simulations on the ion atmosphere contribution to the thermodynamics of λ repressor–operator complex formation. *J. Amer. Chem. Soc.* **113**, 5211–5215.

Jen-Jacobsen, L., Kurpiewski, M., Lesser, D., Grable, J., Boyer, H. W., Rosenberg, J. M. & Greene, P. J. (1983). Coordinate ion pair formation between *Eco*RI endonuclease and DNA. *J. Biol. Chem.* **258**, 14638–14646.

Jen-Jacobsen, L., Lesser, D. & Kurpiewski, M. (1986). The enfolding arms of *Eco*RI endonuclease: role in DNA binding and cleavage. *Cell*, **45**, 619–629.

Jordan, S. R. & Pabo, C. O. (1988). Structure of the lambda complex at 2·5 Å resolution: details of the repressor–operator interactions. *Science*, **242**, 893–898.

Kim, Y., Grable, J. C., Love, R., Greene, P. J. & Rosenberg, J. M. (1990). Refinement of *Eco*RI endonuclease crystal structure: a revised chain tracing. *Science*, **249**, 1307–1309.

Klapper, I., Hagstrom, R., Fine, R., Sharp, K. & Honig, B. (1986). Focusing of electric fields in the active site of CuZn superoxide dismutase: effects of ionic strength and amino acid modification. *Proteins: Struct. Funct. Genet.* **1**, 47–59.

Koblan, K. S. & Ackers, G. K. (1991*a*). Cooperative protein–DNA interactions: effects of KCl on lambda cI binding to OR. *Biochemistry*, **30**, 7822 7827.

Koblan, K. S. & Ackers, G. K. (1991*b*). Energetics of subunit dimerization in bacteriophage lambda cI repressor: linkage to protons, temperature and KCl. *Biochemistry*, **30**, 7817–7821.

Lesser, D. R., Kurpiewski, M. R. & Jen-Jacobsen, L. (1990). The energetic basis of specificity in the *Eco*RI endonuclease–DNA interaction. *Science*, **250**, 776–785.

Lohman, T. M., deHaseth, P. L. & Record, M. T. (1980). Pentalysine-deoxyribonucleic acid interactions: a model for the general effects of ion concentrations on the interactions of proteins with nucleic acids. *Biochemistry*, **19**, 3522–3530.

Manning, G. S. (1969). Limiting laws and counterion condensation in polyelectrolyte solutions. I. Colligative properties. *J. Chem. Phys.* **51**, 924–933.

Manning, G. S. (1978). The molecular theory of polyelectrolyte solutions with applications to the electrostatic properties of polynucleotides. *Quart. Rev. Biophys.* **11**, 179–246.

Marcus, R. A. (1955). Calculation of thermodynamic properties of polyelectrolytes. *J. Chem. Phys.* **23**, 1057–1068.

Martin, K. J. & Schlief, R. F. (1987). Equilibrium DNA-binding of araC protein. Compensation for displaced ions. *J. Mol. Biol.* **195**, 741–744.

McClarin, J. A., Frederick, C. A., Wang, B., Greene, P. G., Boyer, H. W., Grable, J. & Rosenberg, J. M. (1986). Structure of the DNA-*Eco*RI endonuclease recognition complex at 3·0 Å resolution. *Science*, **234**, 1526–1541.

Misra, V. K., Sharp, K. A., Friedman, R. A. & Honig, B. (1994). Salt effects on ligand-DNA binding: minor groove binding antibiotics. *J. Mol. Biol.* **238**, 245–263.

Modrich, P. (1982). Studies on sequence recognition by type II restriction and modification enzymes. *CRC Crit. Rev. Biochem.* **13**, 287–323.

Murthy, C. S., Bacquet, R. J. & Rossky, P. J. (1985). Ionic distributions near polyelectrolytes. A comparison of theoretical approaches. *J. Phys. Chem.* **89**, 701–710.

Nelson, H. C. M. & Sauer, R. T. (1985). Lambda repressor mutations that increase the affinity and specificity of operator binding. *Cell*, **42**, 549–558.

Nicholls, A. & Honig, B. (1991). A rapid finite difference algorithm, utilizing successive over-relaxation to solve the Poisson–Boltzmann equation. *J. Comp. Chem.* **12**, 435–445.

Pabo, C. O., Sauer, R. T., Sturtevant, J. & Ptashne, M. (1979). The lambda repressor contains two domains. *Proc. Nat. Acad. Sci., U.S.A.* **76**, 1608–1612.

Ptashne, M. (1987). *A Genetic Switch. Gene Control and Phage λ*. Blackwell Scientific Publications & Cell Press, Cambridge.

Ralston, M. L. & Jennrich, R. I. (1978). DUD: a derivative-free algorithm for nonlinear least squares. *Technometrics*, **20**, 7–14.

Record, M. T., Lohman, T. M. & deHaseth, P. (1976). Ion effects on ligand–nucleic acid interactions. *J. Mol. Biol.* **107**, 145–158.

Record, M. T., deHaseth, P. L. & Lohman, T. M. (1977). Interpretation of monovalent and divalent cation effects on the *lac* repressor–operator interaction. *Biochemistry*, **16**, 4791–4796.

Record, M. T., Anderson, C. F. & Lohman, T. M. (1978). Thermodynamic analysis of ion effects on the binding and conformational equilibria of proteins and nucleic acids: the roles of ion association or release, screening, and ion effects on water activity. *Quart. Rev. Biophys.* **11**, 103–178.

Record, M. T., Anderson, C. F., Mills, P., Mossing, M. & Roe, J.-H. (1985). Ions as regulators of protein–nucleic acid interactions *in vitro* and *in vivo*. *Advan. Biophys.* **20**, 109–135.

Record, M. T., Ha, J.-H. & Fisher, M. A. (1991). Analysis of equilibrium and kinetic measurements to determine thermodynamic origins of stability and specificity and mechanism of formation of site-specific complexes between proteins and helical DNA. *Methods Enzymol.* **208**, 291–343.

Reiner, E. S. & Radke, C. J. (1990). Variational approach to the electrostatic free energy in charged colloidal suspensions: general theory for open systems. *J. Chem. Soc. Faraday Trans.* **86**, 3901–3912.

Riggs, A. D., Suzuki, H. & Bourgeois, S. (1970). Lac repressor–operator interaction. I. Equilibrium studies. *J. Mol. Biol.* **48**, 67–83.

Rosenberg, J. M. (1991). Structure and function of restriction endonucleases. *Curr. Opin. Struct. Biol.* **1**, 104–113.

Sarai, A. & Takeda, Y. (1989). λ repressor recognizes the approximately 2-fold symmetric half-operator sequences asymmetrically. *Proc. Nat. Acad. Sci., U.S.A.* **86**, 6513–6517.

SAS Institute, I. (1988). *SAS/PC* release 6.03. Cary, NC:SAS Institute, Inc.

Sauer, R. T., Jordan, S. R. & Pabo, C. O. (1990). Lambda repressor: a model system for understanding protein–DNA interactions and protein stability. *Advan. Protein Chem.* **40**, 1–61.

Senear, D. F. & Ackers, G. K. (1990). Proton-linked contributions to site-specific interactions of lambda cI repressor and OR. *Biochemistry*, **29**, 6568–6577.

Senear, D. F. & Batey, R. (1991). Comparison of operator-specific and nonspecific DNA binding of the lambda cI repressor: [KCl] and pH effects. *Biochemistry*, **30**, 6677–6688.

Sharp, K. A. & Honig, B. (1990*a*). Calculating total electrostatic energies with the nonlinear Poisson–Boltzmann equation. *J. Phys. Chem.* **94**, 7684–7692.

Sharp, K. A. & Honig, B. (1990*b*). Electrostatic interactions in macromolecules: theory and applications. *Annu. Rev. Biophys. Biophys. Chem.* **19**, 301–332.

Terry, B. J., Jack, W. E., Rubin, R. A. & Modrich, P. (1983). Thermodynamic parameters governing interaction of *Eco*RI endonuclease with specific and nonspecific DNA sequences. *J. Biol. Chem.* **258**, 9820–9825.

Vershon, A. K., Liao, S.-M., McClure, W. R. & Sauer, R. T. (1987*a*). Bacteriophage P22 mnt repressor.

DNA binding and effects on transcription *in vitro*. *J. Mol. Biol.* **195**, 311–322.

Vershon, A. K., Liao, S.-M., McClure, W. R. & Sauer, R. T. (1987*b*). Interaction of the bacteriophage P22 arc repressor with operator DNA. *J. Mol. Biol.* **195**, 323–331.

Weiner, S. J., Kollman, P. A., Nguyen, D. T. & Case, D. A. (1986). An all atom force field for simulations of proteins and nucleic acids. *J. Comput. Chem.* **7**, 230–252.

Wilson, R. W., Rau, D. C. & Bloomfield, V. A. (1980). Comparison of polyelectrolyte theories of the binding of cations to DNA. *Biophys. J.* **30**, 317–326.

Winter, R. B. & von Hippel, P. H. (1981). Diffusion-driven mechanisms of protein translocation on nucleic acids. 2. The *Escherichia coli* repressor–operator interaction: equilibrium measurements. *Biochemistry*, **20**, 6948–6960.

Wright, D. J., King, K. & Modrich, P. (1989). The negative charge of Glu111 is required to activate the cleavage center of *Eco*RI endonuclease. *J. Biol. Chem.* **264**, 11816–11821.

Yang, A.-S., Gunner, M. R., Sampogna, R., Sharp, K. & Honig, B. (1993). On the calculation of pK_as in proteins. *Proteins: Struct. Funct. Genet.* **15**, 252–265.

Zacharias, M., Luty, B. A., Davis, M. E. & McCammon, J. A. (1992). Poisson–Boltzmann analysis of the λ repressor–operator interaction. *Biophys. J.* **3**, 1280–1285.

Edited by P. von Hippel

(Received 6 July 1993; accepted 20 January 1994)